


June 01, 2016

# Climate, Black Holes and Vorticity: How on Earth are They Related?

By [George Haller](#)

Transport of water by black-hole eddies in the Southern Ocean 

*Materially advected coherent black-hole eddies in the Southern Ocean, identified from satellite data ranging over 135 days. Video credit: George Haller and the Center for Environmental Visualization, University of Washington.*

In short, they are related through oceanic eddies. Often called the weather of the ocean, eddies are gigantic vortices of swirling water. While they exist across a range of spatial scales, perhaps most fascinating are mesoscale eddies, varying between 100 and 200 km in diameter. These eddies are too large to recognize from a ship or an airplane, but were too small to be visible in early satellite observations of the ocean. It wasn't until the 1960s that they were first recorded due to improved satellite altimetry.

Coherent mesoscale eddies, which keep their integrity for extended times, are envisioned to carry the same water body without substantial leakage and deformation. Coherent fluid transport in the unsteady ocean, however, is not directly observable, and thus one must rely on sporadic observations of transported scalars, such as chlorophyll and temperature, to gain insight into material currents. Some exceptional chlorophyll patches captured by eddies drift in the ocean for up to a year or more (see Figure 1a). The carrier eddies show no substantial mixing with surrounding waters, often creating moving oases for the marine food chain.

## Why and How to Track Eddies?

Amidst concerns over climate change, episodic observations of material transport in the ocean are insufficient, and more quantitative and reliable eddy identification tools are needed. For instance, the Agulhas rings, the largest mesoscale eddies in the ocean (see Figure 1b), are believed to transport warm and salty water from the Indian Ocean across the South Atlantic through the so-called Agulhas leakage, which is reportedly on the rise [3]. The rings might traverse as far as the upper arm of the Atlantic Meridional Overturning Circulation (AMOC), whose potential slowdown due to melting sea ice in a warming climate is of current concern. This rise leads to the generation of more Agulhas rings, possibly weakening the AMOC slowdown [1]. To assess the validity of such hypotheses, one must uncover the exact coherent cores of the Agulhas rings from available observational velocity data.

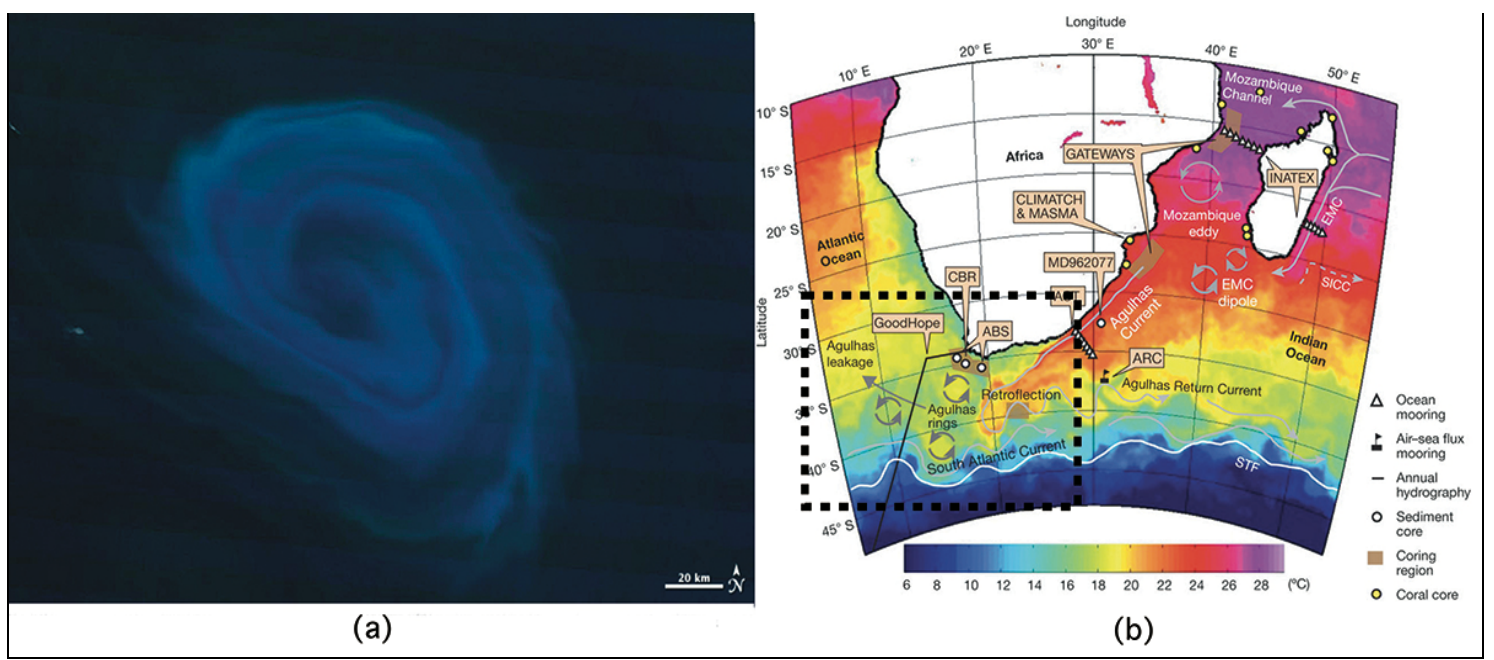


**Figure 1a.** Satellite image of a chlorophyll patch captured by an Agulhas ring. Image credit: NASA Earth Observatory/Jesse Allen. **1b.** A sketch of the Agulhas leakage. Adapted with permission from Macmillan Publishers Ltd.: Nature [1], copyright (2011).

Eddy tracking methods used in oceanography are Eulerian in nature, devised to highlight features of the instantaneous surface velocity field  $v(x, t)$ . The same techniques are nevertheless also broadly believed to identify regions of elliptic (or vortical) trajectories  $x(t)$  for the ordinary differential equation (ODE)  $\dot{x} = v(x, t)$  [4]. Classic examples in the theory of non-autonomous ODEs show that such an inference is generally incorrect, even if  $v$  is just linear in the spatial variable  $x \in \mathbb{R}^2$ . Indeed, it is simple to construct spatially linear unsteady solutions of the Navier–Stokes equation that are pronounced coherent vortices by all instantaneous Eulerian criteria, yet the norm of their trajectories grows exponentially in time [7]. The same effect causes Eulerian eddy tracking methods to overestimate coherent eddy transport in the Agulhas leakage by about an order of magnitude [2].

**Where do Black Holes Come In?**

For unambiguous identification of perfectly coherent material vortices, one first needs a mathematical definition of their boundaries. Such a Lagrangian boundary should show no filamentation over a finite time interval  $[t_0, t]$ , in contrast to the intense and inhomogeneous deformation of material surfaces in turbulent waters outside the vortices. Using elementary continuum mechanics, one finds that the parametrized initial position  $x_0(s)$  of such a coherent boundary must be a closed stationary curve of the averaged relative stretching functional

$$Q_{t_0}^t(\gamma) = \frac{1}{\sigma} \int_0^\sigma \frac{\sqrt{\langle x'_0(s), C_{t_0}^t(x_0(s))x'_0(s) \rangle}}{\sqrt{\langle x'_0(s), x'_0(s) \rangle}} ds,$$

with  $C_{t_0}^t = [\nabla F_{t_0}^t]^T \nabla F_{t_0}^t$  denoting the right Cauchy-Green strain tensor [6]. An argument utilizing Noether’s theorem then implies that closed stationary curves of  $Q_{t_0}^t$  are precisely the closed null-geodesics of the Lorentzian metric tensor family  $E_\lambda(x_0) = \frac{1}{2}[C_{t_0}^t(x_0) - \lambda^2 I]$ , parametrized by  $\lambda \in \mathbb{R}^+$  [9].

This result reveals a surprising mathematical analogy between black holes in general relativity and vortices in the two-dimensional ocean [10]. In the former setting, a photon sphere is a nowhere space-like hypersurface of null-geodesics in space-time, with space-like projections that trap photons orbiting around a black hole forever [5]. In the context of the two-dimensional oceanic space-time, vortex boundaries take the role of such photon spheres. This then implies [9] that a metric singularity of  $E_\lambda(x_0)$  must necessarily arise inside oceanic eddies (see Figure 2), just as metric singularities are believed to arise invariably inside black holes. So, at the level of a mathematical analogy, a material vortex to a two-dimensional ocean matches what a black hole is to Einstein’s four-dimensional space-time.

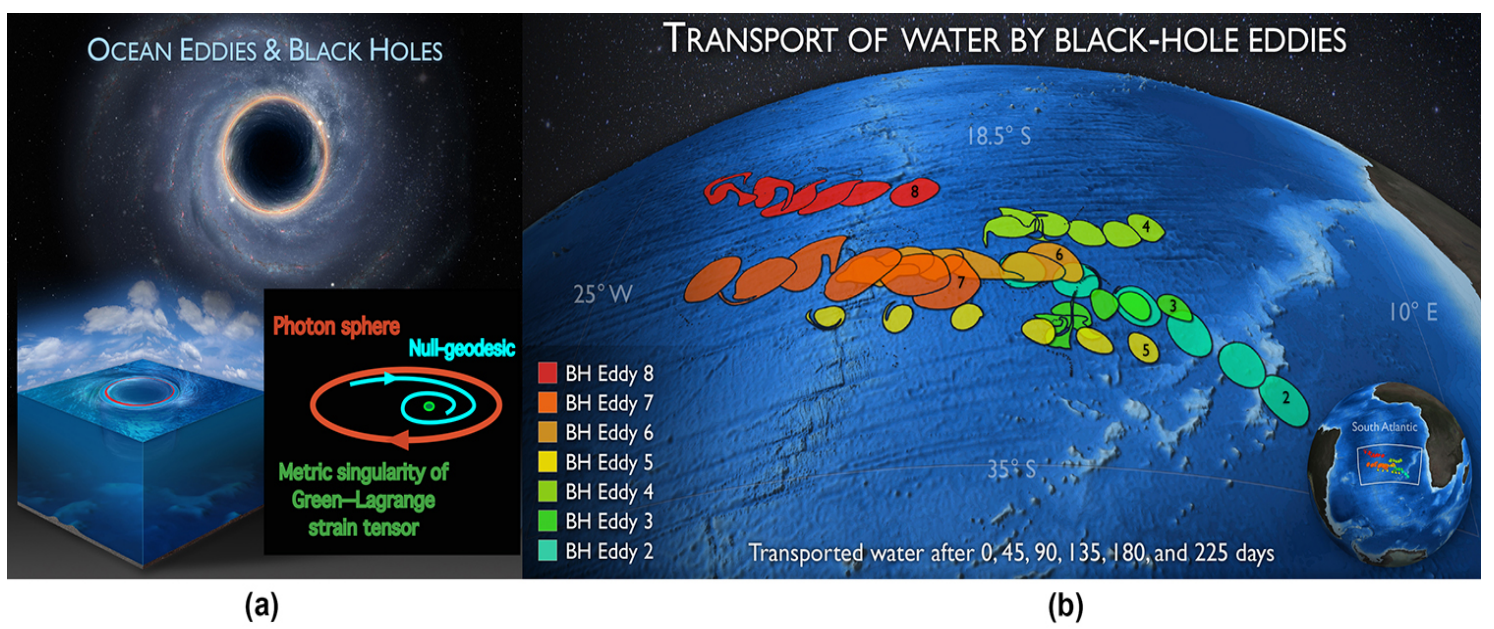


**Figure 2a.** Closed null-geodesics of the two-dimensional generalized Green-Lagrange strain tensor are analogous to photon spheres in the four-dimensional space-time. **2b.** Materially advected coherent black-hole eddies in the Southern Ocean, identified from satellite data ranging over 135 days (details in [9]). See animation above. Image credit: George Haller and the Center for Environmental Visualization, University of Washington.

Beyond providing a curious analogy, metric singularities of the generalized Green-Lagrange strain tensor  $E_\lambda$  form the cornerstone of automated Lagrangian vortex detection schemes for large ocean data sets [13]. Figure 2a shows the evolution of black-hole type vortices in the South Atlantic, computed as null-geodesics encircling metric singularities of  $E_\lambda$  [10]. The flow map  $F_{t_0}^{t_0+135 \text{ days}}$  is computed by integration from a satellite-altimetry-based surface velocity field  $v(x, t)$ .

### Aren't Vortices Supposed to be Related to Vorticity?

They are, but there is a caveat. An important axiom of continuum physics is that material behavior, including material transport by vortices, cannot depend on the observer describing the behavior.

Thus, a self-consistent definition of material eddies must be invariant under all Euclidean observer changes of the form  $x = R(t)X + b(t)$ , where  $R(t)$  is a proper orthogonal tensor family and  $b(t)$  is an arbitrary translation family. While the functional  $Q_{t_0}^t$  defining black-hole eddies is objective, the vorticity  $\omega(x, t) = \nabla \times v(x, t)$  is not. Indeed, an observer change gives the transformed vorticity

$$\tilde{\omega}(\tilde{x}, t) = R^T(t)\omega(x, t) + \dot{r}(t),$$

with the vector  $\dot{r}$  denoting the angular velocity of the frame rotation induced by  $R(t)$ . Because of this  $\dot{r}$  term, the vorticity vector fails to transform properly, as a vector under a linear operator  $R$  would. For this reason, vorticity has long been absent from the toolkit of objective Lagrangian [7] and even Eulerian [12] coherent structure detection.

A recent extension of the classic polar decomposition to non-autonomous processes, however, reveals an intrinsic connection between vorticity and objective material rotation. Valid in any finite dimensions, the *dynamic polar decomposition* theorem [8] guarantees a unique factorization of the flow gradient as

$$\nabla F_{t_0}^t = \Phi_{t_0}^t \Theta_{t_0}^t M_{t_0}^t,$$

where the *dynamic stretch tensor*  $M_{t_0}^t$  is the flow gradient of a purely straining flow; the *mean rotation tensor*  $\Theta_{t_0}^t$  is the flow gradient of a spatially uniform rigid-body rotation; and the *relative rotation tensor*  $\Phi_{t_0}^t$  is the flow gradient of the local deviation from that mean rotation. The material rotation angle generated by  $\Phi_{t_0}^t$  about its time-varying axis of rotation turns out to be a frame-invariant quantity. This objective rotation angle is surprisingly simple to compute: it is given by the Lagrangian-Averaged Vorticity Deviation (LAVD),

$$\text{LAVD}_{t_0}^t(x_0) = \int_{t_0}^t |\omega(x(s; x_0), s) - \bar{\omega}(s)| ds,$$

with  $\omega(t)$  denoting the spatial mean of the vorticity [11].

Defining rotationally-coherent eddy boundaries as surfaces evolving from outermost tubular level sets of the LAVD provides the long-sought link between objective material eddies and vorticity. Unlike black-hole vortices, LAVD-based vortices may exhibit small tangential filamentation in their boundaries (see Figure 3a). The filaments, however, are bound to rotate with the material vortex without large-scale fingering into the surrounding turbulent waters. Figure 3b shows a three-dimensional example of this, with the velocity field generated by the Southern Ocean State Estimate (SOSE) model [14]. Material advection of this remarkably detailed material vortex boundary confirms the rotational coherence guaranteed by the *dynamic polar decomposition* (see animation below).

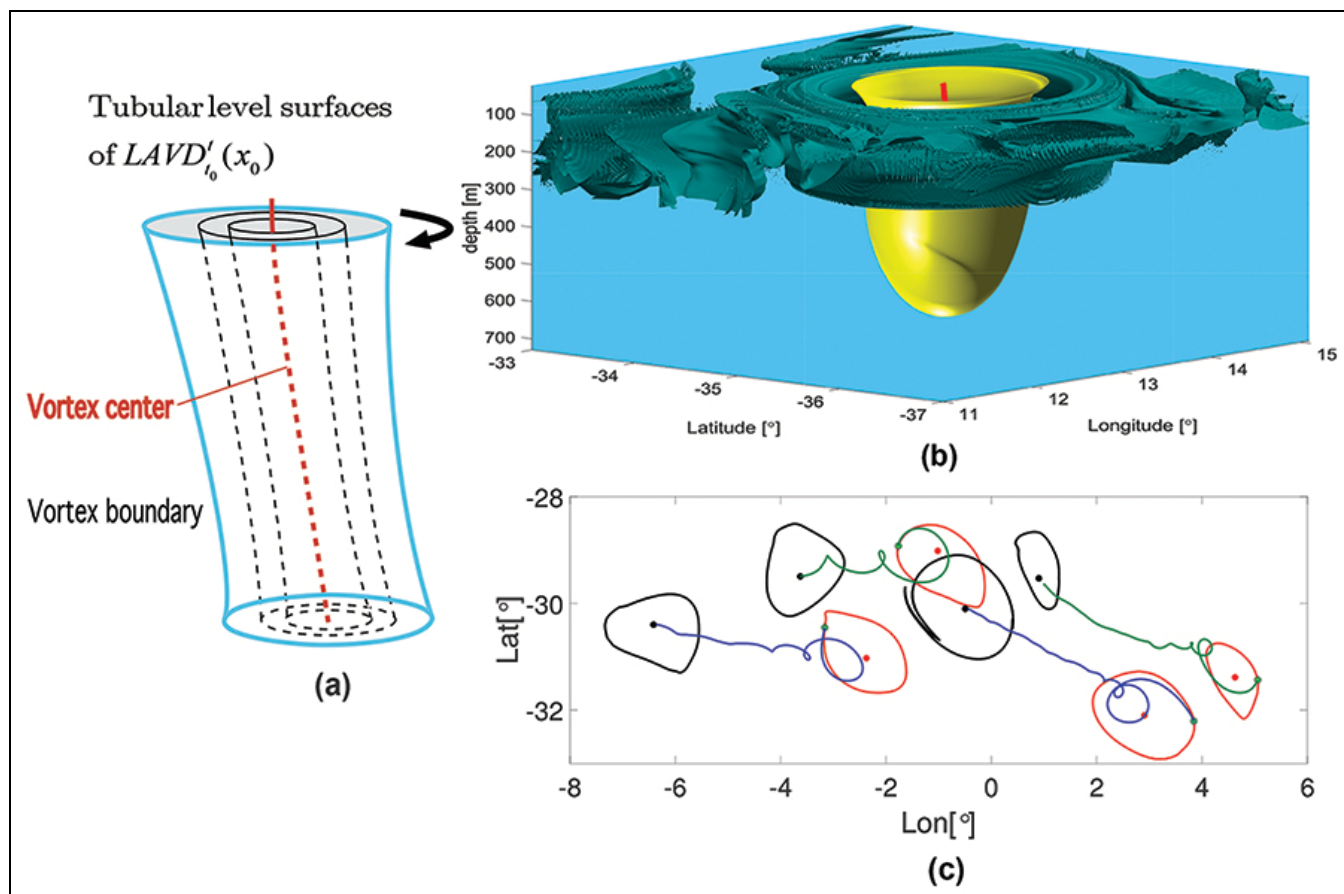
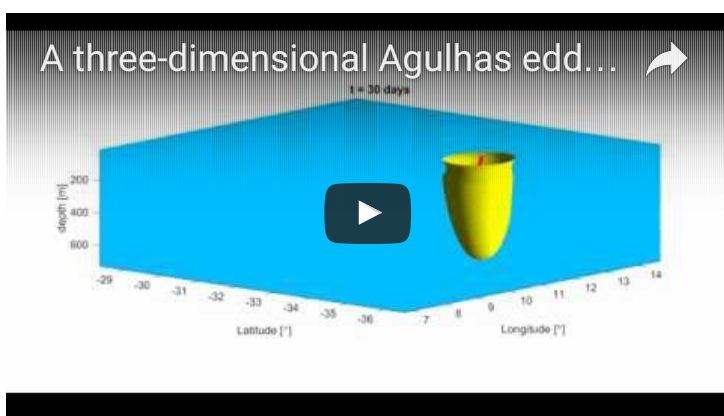


**Figure 3a.** Rotationally coherent vortex boundary and center defined from the LAVD. Image credit: George Haller. **3b.** A three-dimensional Agulhas eddy boundary and eddy center (details in [11]). **3c.** Initial (red) and final (black) advected positions of LAVD-based Agulhas eddies over a period of three months. Floating objects (blue) converge to the centers of anti-cyclonic eddies; sinking objects (green) converge to the centers of cyclonic eddies (details in [11]). See animation below. Image credit for 3b and 3c: Alireza Hadjighasem, ETH Zürich.

Remarkably, singular level sets at the core of nested tubular LAVD levels define vortex centers that can be proven to coincide exactly with the observed cyclonic repellers and anti-cyclonic attractors for positively buoyant inertial particles [11]. Hence, LAVD-based eddy centers are precisely the mysterious drifting locations that collect floating debris in the ocean. Figure 3c shows a numerical verification of this analytic prediction.

Tracking the Agulhas eddies over ... ➔



The animation to the left shows the initial and final advected positions of the Lagrangian-Averaged Vorticity Deviation (LAVD)-based Agulhas eddies over a period of three months. The animation on the right shows a three-dimensional Agulhas eddy boundary and eddy center. Video credit: Alireza Hadjighasem.

Implementing these mathematical advances in *in situ* analysis of the ocean and the atmosphere is an exciting perspective. Beyond quantifying mesoscale eddy transport, black-hole and LAVD eddies of smaller scales could aid real-time decision making in environmental disasters (e.g. oil spills) or in search and rescue operations. On the other extreme of the eddy scale spectrum, these techniques offer a frame-indifferent identification of gigantic material vortices in the atmospheres of other planets, such as Jupiter's Great Red Spot [6]. The quest to uncover coherent oceanic eddies has already led to unexpected links to Lorentzian geometry and continuum mechanics, both of which deserve further exploration.

## References

- [1] Beal, L.M., De Ruijter, W.P.M., Biastoch, A., Zahn, R., & SCOR/WCRP/IAPSO Working Group 136. (2011). On the role of the Agulhas system in ocean circulation and climate. *Nature*, 472, 429–436.
- [2] Beron-Vera, F.J., Wang, Y., Olascoaga, M.J., Goni, J.G., & Haller, G. (2013). Objective detection of oceanic eddies and the Agulhas leakage. *J. Phys. Oceanogr.*, 43, 1426–1438.
- [3] Biastoch, A., Beal, L.M., Casal, T.G.D., & Lutjeharms, J.R.E. (2009). Variability and coherence of the Agulhas Undercurrent in a high-resolution ocean general circulation model. *J. Phys. Oceanogr.*, 39, 2417–2435.
- [4] Chelton, D.B., Gaube, P., Schlax, M.G., Early, J.J., & Samelson, R.M. (2011). The influence of nonlinear mesoscale eddies on near-surface oceanic chlorophyll. *Science*, 334, 328–332.
- [5] Claudel, C-M., Virbhadra, K.S., & Ellis, G.F.R. (2001). The geometry of photon surfaces. *J. Math. Phys.*, 42, 818–838.
- [6] Hadjighasem, A., & Haller, G. (2016). Geodesic transport barriers in Jupiter's atmosphere: a video-based analysis. *SIAM Review*, 58, 69–89.
- [7] Haller, G. (2015). Lagrangian Coherent Structures. *Annual Rev. Fluid. Mech.*, 47, 137–162.
- [8] Haller, G. (2016). Dynamically consistent rotation and stretch tensors from a dynamic polar decomposition. *J. Mech. Phys. Solids*, 80, 70–93.
- [9] Haller, G., & Beron-Vera, F.J. (2013). Coherent Lagrangian vortices: The black holes of turbulence. *J. Fluid Mech.*, 731, R4.
- [10] Haller, G., & Beron-Vera, F.J. (2014). Addendum to 'Coherent Lagrangian vortices: the black holes of turbulence.' *J. Fluid. Mech.*, 755, R3.
- [11] Haller, G., Hadjighasem, A., Farazmand, M., & Huhn, F. (2016). Defining coherent vortices objectively from the vorticity. *J. Fluid Mech.*, 795, 136–173.
- [12] Jeong, J., & Hussein, A.K.M.F. (1995). On the identification of a vortex. *J. Fluid Mech.*, 285, 69–94.
- [13] Karrasch, D., Huhn, F., & Haller, G. (2014). Automated detection of coherent Lagrangian vortices in two-dimensional unsteady flows. *Proc. Royal Society*, 471, 20140639.
- [14] Mazlo, M.R., Heimbach, P., & Wunsch, C. (2010). An Eddy-Permitting Southern Ocean State Estimate. *J. Phys. Oceanogr.*, 40, 880–899.

*George Haller is a professor of mechanical engineering at ETH Zürich, where he holds the Chair in Nonlinear Dynamics. Among other interests, he has been working on the mathematics of coherent structures in unsteady flow data for the past two decades.*